

Mirages and Large TeV Halo-Pulsar Offsets from Cosmic Ray Propagation

Yiwei Bao^{1,2}, Gwenael Giacinti^{2,3,*}, Ruo-Yu Liu^{1,4,†}, Hai-Ming Zhang¹, and Yang Chen^{1,4‡}

¹*Department of Astronomy, Nanjing University, 163 Xianlin Avenue, Nanjing 210023, China*

²*Tsung-Dao Lee Institute, Shanghai Jiao Tong University, Shanghai 201210, China*

³*School of Physics and Astronomy, Shanghai Jiao Tong University, Shanghai 200240, China*

⁴*Key Laboratory of Modern Astronomy and Astrophysics,
Nanjing University, Ministry of Education, Nanjing, China*

(Dated: July 3, 2024)

The study of extended γ -ray sources usually assumes symmetric diffusion of cosmic rays. However, recent observations of multiple sources near single pulsars and significant offsets between TeV halo centroids and their parent pulsars suggest that this assumption is overly simplistic. In this Letter, we demonstrate that asymmetric propagation of cosmic rays near their accelerators may create multiple TeV sources instead of a single symmetric source. This mechanism also explains the large offsets between TeV halo centroids and their pulsars. We demonstrate that several perplexing detected sources can be naturally explained without invoking additional invisible accelerators.

Introduction— HAWC [1] and LHAASO [2] have detected almost a hundred gamma-ray sources at TeV energies and beyond. Many of these sources are extended and likely due to inverse Compton (IC) from relativistic electrons. One prominent and intriguing example of such leptonic sources is the “TeV halo”. TeV halos are extended gamma-ray emitting regions around middle-aged pulsars. They are due to electrons with energies up to about a PeV [3–5], and with typical spatial extensions of the order of ≈ 50 pc. Within these regions, the diffusion coefficient of cosmic rays (CRs) is suppressed by a factor of 10^2 – 10^3 compared with the value derived from the Boron-to-Carbon ratio [6]. Studying TeV halos not only provides insights into these unique celestial phenomena but also offers valuable information about the turbulent magnetic fields in the interstellar medium around these middle-aged pulsars [7].

The LHAASO catalog identifies dozens of TeV sources that are associated with middle-aged pulsars, and like in HESS and HAWC observations [1], a large fraction of these sources exhibit significant offsets between their centroids and the positions of the pulsars. These offsets, however, can neither be explained by the interaction of the reverse shock with the pulsar wind nebula (PWN) [8], nor by the proper motion of the pulsar when > 10 TeV γ -rays are considered [9]. Moreover, some of these extended sources are not even circularly symmetric. Notable examples include 1LHAASO J0206+4302u and 1LHAASO J0212+4254u. These discoveries challenge the traditional cosmic-ray diffusion model, which predicts that the accelerator should always be located at the center of the observed emission and that the radial profile of the source should be a symmetric Gaussian—or an elliptical Gaussian if anisotropic diffusion along a large-scale magnetic field is considered.

In reality, cosmic-ray propagation is expected to be very filamentary on scales smaller than the coherence length of the turbulence, because these particles follow their local magnetic field lines [10]. In contrast, stan-

dard diffusion models approximate their propagation as isotropic or anisotropic diffusion, with a homogeneous diffusion coefficient or tensor around their sources. This approximation is valid only if the diffusion length scale is much larger than the coherence length L_c of the magnetic field ($\approx 1/5$ of the outer scale of the turbulence for a Kolmogorov spectrum), with the specific influence of given magnetic field structures averaging out thanks to the particle traversing many different field structures whose directions are random. As a result, in such models, the extended gamma-ray source will always be centered at the particle accelerator. In practice, this phenomenological approximation is often sufficient, because the coherence length in spiral arms—where most pulsars are located—may be as low as 2 pc [11], and the lifetime of low-energy electrons is sufficiently long to allow them to cross several coherence lengths. However, challenges have now started to arise as more sources have been discovered above 20 TeV in the inter-arm regions (where the coherence length may be much larger [11]) and off-plane regions (where the average coherence length could reach around 200 pc [12]). For such sources, the diffusion approximation is expected to break down because their electrons can only propagate within a coherence length. Hence, it is necessary to treat electron propagation in a more realistically way to explain their extended gamma-ray emissions. As shown below, if the magnetic field is bent away from or towards the observer, the electrons accumulate along the line of sight, forming apparent, off-centered gamma-ray sources, whose directions on the sky may be far from that of the true parent electron source. Due to their misleading nature, we call them “mirage sources”, although the underlying physics is different from that of optical mirages. For this new type of gamma-ray sources, no astrophysical accelerators lie at their centroids, which is dramatically at odds with any naive or standard expectation. The electrons responsible for the detected sources have, in fact, been accelerated in a nearby accelerator, which may even be located outside

the detected gamma-ray source.

In this Letter, instead of adopting the traditional diffusion approximation to investigate electron propagation around their sources, we calculate from first principles the motion of individual electrons in synthetic three-dimensional turbulence. The latter approach can give vastly different results, and it is more realistic because the (effective) cosmic-ray diffusion tensor strongly varies in space on length scales that are smaller than the coherence length. Our method is more fundamental and more flexible than using the diffusion approximation. Indeed, it can both resolve the filamentary propagation of electrons on small scales, and recovers the predictions from the diffusion approximation on large scales. By considering the short lifetime of $\gtrsim 100$ TeV electrons, we find that the real distribution of these electrons around their sources can be very filamentary even in strong turbulent magnetic fields. Also, we find that both the presence of large offsets from the pulsars and the presence of mirage sources are two interlinked phenomena arising from this filamentary propagation. Our results suggest that in the inter-arm region and in the Galactic halo where the coherence length is large, a large pulsar halo could be identified as multiple distinct smaller halos. Moreover, when the primary identified halo exhibits low luminosity, these ancillary mirage halos could emerge as the sole identified entities, leading to considerable offsets between the detected gamma-ray sources and the actual astrophysical source of the electrons.

Methods— We use test particle simulations, where we integrate the trajectories of > 100 TeV electrons in a turbulent magnetic field, as in e.g. Refs. [13–15]. For the trajectory integrator, we use the original Boris pusher [16]. These electrons display an inverse Compton (IC) spectrum mainly off the cosmic microwave background (CMB), peaking around 20 TeV. For the magnetic field, we use the combination of a regular component \mathbf{B}_r and a turbulent component \mathbf{B}_t which can be expressed by a superposition of N_m plane waves [13]. Hereafter, we adopt $N_m = 600$, over 6 orders of magnitude in wavelength. The electrons are injected at a point source in the simulation, assumed to be a pulsar, and with a power-law spectrum $dN/d\gamma \propto \gamma^{-\alpha}$, where N denotes the electron number and $\alpha \approx 2$ the power-law index. The spin-down luminosity of the pulsar is represented as $L(t) = L_0/[1 + (t/\tau_0)^2]$, with L_0 the initial spin-down luminosity and τ_0 the initial spin-down timescale. To mimic the continuous injection of electrons, we inject $\approx 10^4$ numerical particles continuously over time with energy $\gamma(t_{\text{inj}}) = \int_{t_{\text{age}}}^{t_{\text{inj}}} [\dot{\gamma}_{\text{sync}}(\gamma) + \dot{\gamma}_{\text{IC}}(\gamma)] + 100 \text{ TeV}/m_e c^2$. This ensures that they are all cooled down to 100 TeV at the time t_{age} , where t_{inj} is the injection time of the particle and t_{age} the current age of pulsar. The value of t_{inj} is set such that every numerical particle represents roughly the same number of real electrons. We only study here sources located within a few kpc from the Sun, due to

their better detectability. Therefore, for the seed photon energy density, we use the interstellar radiation field averaged over a 2 kpc region surrounding the Sun.

For the simulation data analysis, we assume that the TeV halos generated by these pulsars are observed by LHAASO KM2A [17]. We consider the observations to be at 20 TeV, and we set here the reference luminosity of the pulsar halo to $L_{\text{ref}} = 6 \times 10^{32}$ erg/s. This γ -ray luminosity is about 6 times that of the observed luminosity of Geminga’s halo in the range of 8–40 TeV [6], but still reasonable. A wider range of luminosities is explored in [18] (paper II). For fainter sources, the lower luminosity can be compensated by an increase in observation time. Assuming all arriving photons to be at 20 TeV, the resulting annual counts is $8.1 \times 10^5 (250 \text{ pc } d^{-1})^2$ (with d being the distance to the pulsar). Our background is set to be consistent with that in the Crab Nebula region, which results in 1 event per hour within a 1° cone [5]. We set the observation time to 3 yr, which is roughly the LHAASO effective operation time, and we assume that the source is visible for 6 hours per day.

For smoothing, we apply a point spread function (PSF) of 0.3° (LHAASO KM2A resolution at 20 TeV [17]). The fraction of total counts in each bin is computed by summing the Gaussian of 10240 numerical particles in each observation bin (of 0.1°). We employ the standard “on-off method” for analyzing these observational counts as is used by the LHAASO Collaboration.

Multiple sub-halos and large TeV halo-pulsar offsets— In our simulations, we frequently detect multiple halo-like sources forming near a single accelerator. The underlying reason for having such multiple sources is that when the electrons diffuse along magnetic field lines, these magnetic field lines bend on scales comparable with the coherence length. When these bent field lines align roughly with our line of sight, a projection effect occurs, causing the electrons to accumulate along the line of sight and to produce a mirage source.

The offsets observed in the data between TeV halo centroids and pulsars locations can also be attributed to this phenomenon of mirage sources. More precisely, if the primary halo that is closer to the pulsar happens to be dimmer than its adjacent halos, the main halo may become elusive, and might even drown in the background noise. As a result, the only detectable halo could be the brighter adjacent one, resulting in a surprisingly large apparent offset between the detected TeV halo and the location of its parent pulsar.

In paper II, we investigate how mirage source properties are influenced by the regular-to-turbulent magnetic field strength ratio. Provided that this ratio B_r/B_t is $\lesssim 1$ (we explore up to 3, higher ratio is not realistic in the Galaxy), it does not significantly impact the properties of mirage sources. Therefore, in the following, we will not further discuss the impact of B_r/B_t .

In Figure 1, the particles are injected at the center

of each panel at (0,0), in two different realisations of the magnetic turbulence with $L_c = 40$ pc, $B_r = 0$ and $B_t = 3 \mu\text{G}$. The distance of the pulsar is set to 250 pc. The colors represent the gamma-ray emission from these sources, and the noise is not displayed. One can see that a source forms near the injection site in each panel (orange dot for its centroid). Along the filamentary magnetic field, we also detect two other sources with similar brightness (black and green dots). Therefore, a single large halo can be very filamentary and can potentially be identified as triple Gaussian sources lying along the filamentary structure.

In Figure 2, two configurations with very large offsets are displayed. As can be seen, the main sources near the parent pulsars could have half of the surface brightness of the secondary sources. With noises taken into consideration, we may only see the secondary sources, with the main sources being drowned in the noise. In these two panels, we put the sources at a distance of 1 kpc (at larger distance the offsets would be even more obvious, because the brightness ratio of two sources are the same, and the main sources are more easily buried by the noise), and the parameters are set to $L_c = 200$ pc (the mean Galactic value according to [12]), $B_r = 0$ and $B_t = 0.5 \mu\text{G}$ (a reasonable turbulent field strength, see table of paper II).

Applications— Despite their complicated evolution in their early ages, a large fraction of pulsar wind nebulae (PWNe) will ultimately evolve into a bow shock pulsar wind nebula (BSPWNe) in the interstellar medium (ISM) due to their high kick velocity ($100\text{--}500 \text{ km s}^{-1}$ [19]). This transition is a result of the constant proper motion velocity of the pulsar over time and the significantly decreasing expansion velocity of the supernova remnants. Consequently, these pulsars will eventually leave their parent SNRs and move supersonically in the ISM. In Figure 3, we show three configurations which can reproduce the sources 1LHAASO J0206+4302u and 1LHAASO J0212+4254u. The offset from 1LHAASO J0206+4302u to the millisecond pulsar J0218+4232 can be attributed to the BSPWN whose tail can extend for tens of pc before it gets destroyed by neutral mass loading [20, 21]. The real separation of the two sources is ≈ 70 pc, and the resulting required L_c would be ~ 280 pc, which is reasonable at high Galactic latitude. In the first panel, $L_c = 200$ pc, and the injection is isotropic. In the other panels, $L_c = 400$ pc, and all electrons have an initial positive y velocity to mimic the particle injection at the tail of the BSPWN. The phenomenon is more obvious with narrower injection. The total γ -ray luminosity is roughly 10 times that of Geminga. Parameters are set to $B_r = 0.7 \mu\text{G}$ and $B_t = 0.7 \mu\text{G}$ (see paper II for the turbulent and regular field strength at the location of PSR J0218+4232). With the observed γ -ray index ≈ 2.5 , we use $\alpha = 1.76$, and the distance is set to be $d = 3$ kpc (distance of the milli-second pulsar). Meanwhile, Faraday rotation measurements have revealed a

large-scale magnetic field parallel to the Galactic plane [22], which is consistent with our study here because 1LHAASO J0206+4302u and 1LHAASO J0212+4254u lie almost parallel to the Galactic disk.

The electron density inside the BSPWN tail is extremely low, and therefore the tail can hardly be seen. The injection of the electrons could happen at the end of the BSPWN tail, as in the traditional picture, or everywhere around the BSPWN [23]. The latter explanation can hardly explain the offset, and we then adopt the traditional scenario. The combined flux of all the sub-sources perceived by KM2A, is $0.54 \times 10^{-16} \text{ cm}^{-2} \text{ s}^{-1} \text{ TeV}^{-1}$ [2].

Meanwhile, using this model, the offsets observed in many TeV halos can be naturally accounted for, such as J2005+3415 and J2005+3050 (see paper II for detailed calculations).

Discussion— Even though mirage sources look similar to real sources, it is possible to identify them as mirages. The most intrinsic feature of a mirage source is that there is always a connecting structure in gamma-rays (probably slightly dimmer than the sources in TeV) connecting the pulsar and the mirage source. Although with current observations the connecting structure may be drowned in the noise, it might be possible to detect it in the future with a larger observation time, or with experiments with better sensitivities.

It is also possible to distinguish mirage halos thanks to observations in other wavelengths. The magnetic flux tube in the halo is oriented nearly along the line of sight, resulting in the synchrotron emission from the electrons being mainly emitted perpendicular to the line of sight. Therefore, mirage sources are expected to be very faint in X-rays, compared to their γ -ray luminosity. On the other hand, the thin structure connecting the primary source to the mirage sources should be brighter in X-rays and easier to detect, also because of the orientation of the magnetic fields. In contrast, if the gamma-ray sources are contributed by invisible radio-quiet pulsars, there should be no structures connecting the pulsars and the offsetted sources, and there will be a small X-ray PWN surrounding the very vicinity of the pulsar, just like the Geminga PWN [24]. Therefore, future X-ray telescopes with low sensitivities could help confirm whether the source is a mirage, or is contributed by a radio-quiet invisible pulsar.

When the source is bright, the asymmetry increases the number of detected sources, and when the source is dim, the asymmetry decreases the number of detected sources because it is harder to identify a source with a standard Gaussian if the source is faint and far away (~ 3 kpc) from us. This helps account for the relatively few detected TeV halos compared to the numerous detected pulsars. However, more sources will become identifiable as observation time increases.

Our simulations use synthetic turbulent magnetic fields based on Ref.[13], and assume isotropic turbulence with

a Kolmogorov power spectrum. However, the properties of the interstellar turbulence may be different, see e.g. [25, 26]. Although probably not accurate at gyration scales, our turbulence does capture well the more isotropic long-wavelength modes in the turbulence, which are those driving the filamentary propagation of cosmic-rays on L_c scales [10], as well as the formation of mirage sources and large offsets. Our method can handle a wide range of turbulence length scales within reasonable computing times. More realistic simulations, like particle-in-cell or 3D magnetohydrodynamic simulations, only cover limited spatial scales, restricting the range of electron energies that can be studied with them.

Conclusions and perspectives— The assumption of isotropic cosmic-ray diffusion, which is traditionally used in the study of TeV halos around pulsars, is getting challenged by recent observations of multiple sources near single pulsars and significant offsets between TeV halo centroids and their parent pulsars. In this Letter, we introduced the novel concept of mirage sources. We demonstrated, by propagating individual electrons from first principles, that the intrinsically asymmetric propagation of electrons around pulsars can create multiple detectable TeV sources instead of a single symmetric TeV halo. This mechanism also explains large offsets between TeV halo centroids and their parent pulsars.

We showed that many perplexing gamma-ray sources can be interpreted through asymmetric propagation very naturally. In particular, one asymmetric halo generated by a pulsar may be identified as multiple sources. Our model explains observed halo-like TeV γ -ray emissions with significant offsets from nearby pulsars. It suggests that these halos may be attributed to those pulsars despite their significant offsets, rather than by invisible radio-quiet pulsars closer to the TeV halo centers. Our results are also consistent with the large scale magnetic field found parallel to the Galactic disk [22]. Our model predicts that new TeV halos discovered at high Galactic latitude, if any, will likely show a filamentary structure and maybe also mirage sources/large offsets.

Acknowledgements- We thank Chunkai Yu, Hao Zhou and Giovanni Morlino for discussion. This work is supported by NSFC under grants No. 12393853, 12350610239, 12393852, 12173018, 12121003 and U2031105.

* gwenael.giacinti@sytu.edu.cn

† ryliu@nju.edu.cn

‡ ygchen@nju.edu.cn

- [1] A. Albert, R. Alfaro, C. Alvarez, J. R. A. Camacho, J. C. Arteaga-Velázquez, K. P. Arumbabu, D. Avila Rojas, H. A. Ayala Solares, V. Baghmany, E. Belmont-Moreno, et al., *Astrophys. J.* **905**, 76 (2020), 2007.08582.
 [2] Z. Cao, F. Aharonian, Q. An, Axikegu, Y. X. Bai, Y. W.

- Bao, D. Bastieri, X. J. Bi, Y. J. Bi, J. T. Cai, et al., *ApJS* **271**, 25 (2024), 2305.17030.
 [3] L. Sironi and A. Spitkovsky, *ApJL* **783**, L21 (2014), 1401.5471.
 [4] B. Cerutti, A. A. Philippov, and G. Dubus, *Astronomy and Astrophysics* **642**, A204 (2020), 2008.11462.
 [5] Lhaaso Collaboration, Z. Cao, F. Aharonian, Q. An, Axikegu, L. X. Bai, Y. X. Bai, Y. W. Bao, D. Bastieri, X. J. Bi, et al., *Science* **373**, 425 (2021), 2111.06545.
 [6] A. U. Abeysekara, A. Albert, R. Alfaro, C. Alvarez, J. D. Álvarez, R. Arceo, J. C. Arteaga-Velázquez, D. Avila Rojas, H. A. Ayala Solares, A. S. Barber, et al., *Science* **358**, 911 (2017), 1711.06223.
 [7] R. López-Coto and G. Giacinti, *Mon. Not. R. Astron. Soc.* **479**, 4526 (2018), 1712.04373.
 [8] P. Slane, I. Lovchinsky, C. Kolb, S. L. Snowden, T. Temim, J. Blondin, F. Bocchino, M. Miceli, R. A. Chevalier, J. P. Hughes, et al., *Astrophys. J.* **865**, 86 (2018), 1808.03878.
 [9] Y. Zhang, R.-Y. Liu, S. Z. Chen, and X.-Y. Wang, *Astrophys. J.* **922**, 130 (2021), 2010.15731.
 [10] G. Giacinti, M. Kachelrieß, and D. V. Semikoz, *Phys. Rev. Lett.* **108**, 261101 (2012), 1204.1271.
 [11] M. Haverkorn, B. M. Gaensler, J. C. Brown, N. S. Bizunok, N. M. McClure-Griffiths, J. M. Dickey, and A. J. Green, *ApJL* **637**, L33 (2006), astro-ph/0512456.
 [12] M. C. Beck, A. M. Beck, R. Beck, K. Dolag, A. W. Strong, and P. Nielaba, *JCAP* **2016**, 056 (2016), 1409.5120.
 [13] J. Giacalone and J. R. Jokipii, *Astrophys. J.* **520**, 204 (1999).
 [14] D. DeMarco, P. Blasi, and T. Stanev, *JCAP* **2007**, 027 (2007), 0705.1972.
 [15] G. Giacinti, M. Kachelrieß, D. V. Semikoz, and G. Sigl, *JCAP* **2012**, 031 (2012), 1112.5599.
 [16] S. Zenitani and T. Umeda, *Physics of Plasmas* **25**, 112110 (2018), 1809.04378.
 [17] F. Aharonian, Q. An, Axikegu, L. X. Bai, Y. X. Bai, Y. W. Bao, D. Bastieri, X. J. Bi, Y. J. Bi, H. Cai, et al., *Chinese Physics C* **45**, 025002 (2021), 2010.06205.
 [18] Y. Bao, R. Liu, G. Giacinti, H. Zhang, and Y. Chen, *Phys. Rev. D*, submitted (2024).
 [19] F. Verbunt, A. Igoshev, and E. Cator, *Astronomy and Astrophysics* **608**, A57 (2017), 1708.08281.
 [20] C. Y. Ng, N. Bucciantini, B. M. Gaensler, F. Camilo, S. Chatterjee, and A. Bouchard, *Astrophys. J.* **746**, 105 (2012), 1109.2233.
 [21] G. Morlino, M. Lyutikov, and M. Vorster, *Mon. Not. R. Astron. Soc.* **454**, 3886 (2015), 1505.01712.
 [22] J. Xu and J. L. Han, *Astrophys. J.* **966**, 240 (2024), 2404.02038.
 [23] B. Olmi, *Universe* **9**, 402 (2023), 2309.02263.
 [24] B. Posselt, G. G. Pavlov, P. O. Slane, R. Romani, N. Bucciantini, A. M. Bykov, O. Kargaltsev, M. C. Weisskopf, and C. Y. Ng, *Astrophys. J.* **835**, 66 (2017), 1611.03496.
 [25] H. Yan and A. Lazarian, *Phys. Rev. Lett.* **89**, 281102 (2002), astro-ph/0205285.
 [26] S. Malik, K. H. Yuen, and H. Yan, *Astrophys. J.* **965**, 65 (2024), 2307.13342.
 [27] M. Aguilar, L. Ali Cavazonza, G. Ambrosi, L. Arruda, N. Attig, S. Aupetit, P. Azzarello, A. Bachlechner, F. Barao, A. Barrau, et al., *Phys. Rev. Lett.* **117**, 231102 (2016).

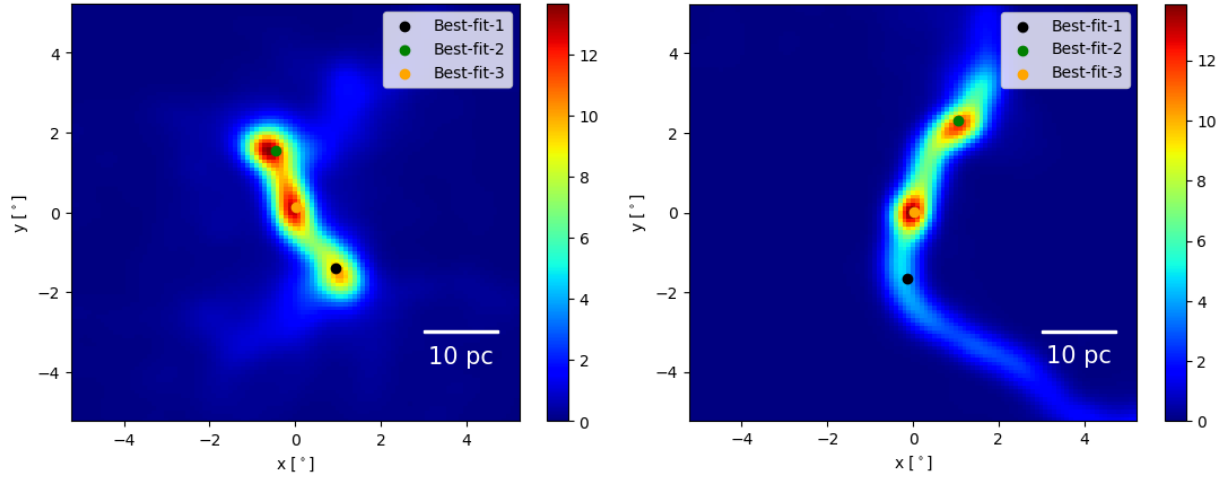


FIG. 1. Cases in which a single halo could potentially be misinterpreted as triple halos. The color representation indicates the number of counts in each grid point (smoothed with Gaussian PSF). The noise has been removed. The best-fit points are the best-fit center of Gaussians, and the particles are injected at (0,0).

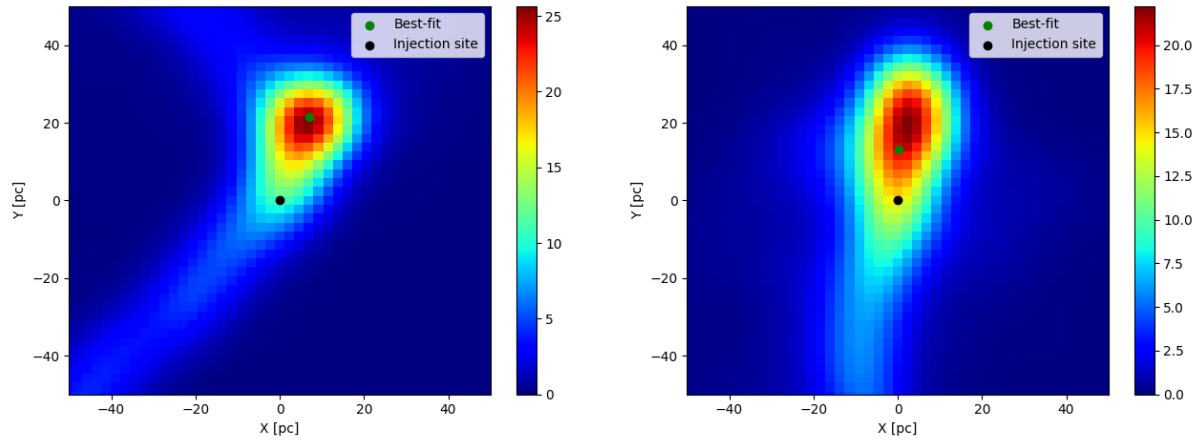


FIG. 2. Cases in which a large offsets can arise from the same mechanism. The color representation indicates the number of counts in each grid point. The noise has been removed.

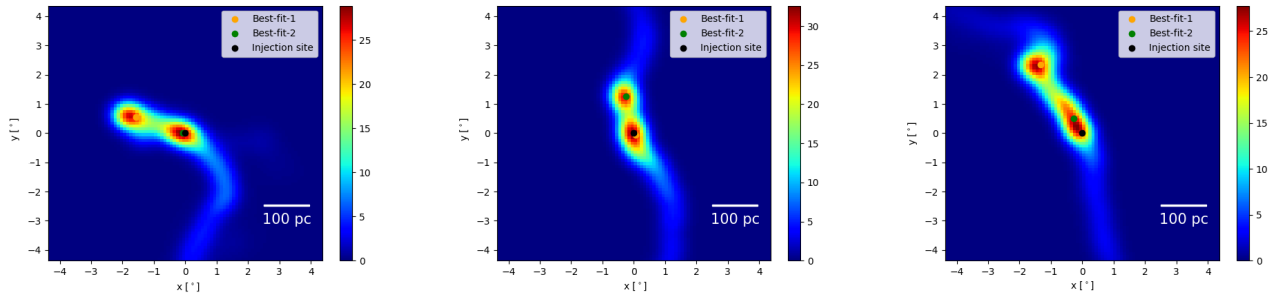


FIG. 3. Three configuration which can reproduce the 1LHAASO J0206+4302u and 1LHAASO J0212+4254u, with the color represent in the number of counts in each grid point. The noise has been removed.

- [28] Q. Yuan, S.-J. Lin, K. Fang, and X.-J. Bi, Phys. Rev. D **95**, 083007 (2017), 1701.06149.
- [29] G. Giacinti, M. Kachelrieß, and D. V. Semikoz, Phys. Rev. D **91**, 083009 (2015), 1502.01608.
- [30] Y. Bao, S. Liu, and Y. Chen, Astrophys. J. **877**, 54 (2019), 1907.02037.
- [31] Y. Bao and Y. Chen, Astrophys. J. **881**, 148 (2019), 1907.02038.